METHODS FOR REDUCING DISPERSION PHENOMENA IN OPTICAL FIBERS

Sh.M. Parpiyeva
Tashkent University of Information Technologies named after Muhammad al-Khwarizmi
https://doi.org/10.5281/zenodo.19722833

Abstract. *This article presents a comprehensive analysis of the dispersion phenomenon in optical fiber communication systems, its physical nature, and its impact on signal transmission performance. Dispersion leads to temporal broadening of optical pulses, resulting in signal distortion, intersymbol interference, and limitations on transmission speed and distance. The study examines the main types of dispersion, including chromatic dispersion (material and waveguide components), modal dispersion, and polarization mode dispersion.*

Special attention is given to the role of dispersion in modern high-speed optical communication systems and its impact on network efficiency. Various dispersion mitigation and compensation techniques are analyzed, such as dispersion compensating fibers (DCF), optical compensators, fiber Bragg gratings, soliton-based transmission, and digital signal processing (DSP) methods. The results demonstrate that effective dispersion management is essential for improving the reliability and capacity of optical communication networks.

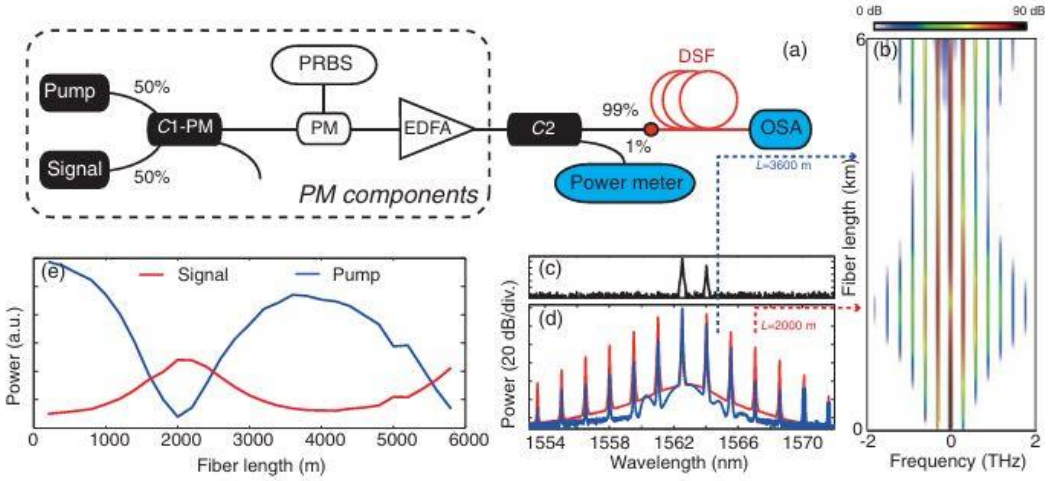
Keywords: *optical fiber communication, dispersion, chromatic dispersion, modal dispersion, polarization mode dispersion, DCF, DSP, solitons, optical networks.*

INTRODUCTION

As a result of the rapid development of modern information and communication technologies, the demand for high-speed and large-volume data transmission has been increasing significantly. In particular, the expansion of internet networks, the advancement of cloud technologies, multimedia services, and the deployment of 5G and next-generation mobile communication systems have further intensified the need for optical fiber communication systems. Optical fiber communication systems are considered superior to other transmission media due to their high bandwidth capacity, low signal loss, and resistance to electromagnetic interference.

At the same time, there are several physical factors that affect the efficient operation of optical fiber communication systems, among which dispersion is one of the most significant. Dispersion leads to the temporal spreading of signal pulses as a result of different wavelength components of the optical signal propagating at different velocities. This phenomenon causes signal distortion, overlap of adjacent pulses, and consequently reduces the accuracy of transmitted data.

Dispersion is particularly a critical issue in high-speed and long-distance optical communication systems. As the transmission speed increases, the duration of pulses becomes shorter, making them more sensitive to the effects of dispersion. As a result, signal distortion occurs more rapidly, leading to a decrease in the overall performance efficiency of the system. Therefore, an in-depth study of dispersion, identification of its types, and the development of effective mitigation methods are among the most important challenges in modern optical communication systems.



In optical fibers, several main types of dispersion exist, among which chromatic dispersion (including material and waveguide dispersion), modal dispersion, and polarization mode dispersion play a significant role. Each type of dispersion affects signal transmission in its own way, and different technological approaches are required to mitigate them effectively In the experimental setup shown in Figure 1(a),

In this experiment, we use two monochromatic tunable diode lasers generating the pump and signal waves, as shown in the upper-left corner of Figure 1. The two optical fields are combined through a polarization-maintaining 50:50 coupler. Each of them is phase-modulated with a 3 Gbit/s pseudo-random bit sequence in order to suppress the stimulated Brillouin scattering (SBS) effect.

Subsequently, the two waves are amplified in an erbium-doped fiber amplifier (EDFA) before being launched into the dispersion-shifted fiber (DSF). To achieve complete matching between the polarization states of the pump and signal waves prior to their injection into the DSF, adjustment is performed using polarization-maintaining components placed before the second coupler, C2. The DSF is similar to that described in Ref. [22]. The total power of the pump and signal launched into the fiber is 27.7 dBm, with a power difference of 11 dB between the pump and the signal.

Figure 1(a) shows the experimental setup. The notations are as follows: C1 and C2 – optical couplers; PRBS – pseudo-random bit sequence; PM – phase modulator; and OSA – optical spectrum analyzer. The experimental results include: (b) the evolution of the spectrum as a function of fiber length; spectra recorded at specific lengths (c) L=0L = 0L=0 m and (d) L=2000L = 2000L=2000 m (red curve) and L=3600L = 3600L=3600 m (blue curve); and (e) the evolution of pump and signal powers along the fiber length. All these experimental results were obtained with a second-order dispersion value of β2=−1.116×10−27 s2/m\beta_2 = -1.116 \times 10^{-27}\ \text{s}^2/\text{m}β2=−1.116×10−27 s2/m (i.e., 11.7 nm above the zero-dispersion wavelength, ZDW).

In other words, PP=530P_P = 530PP=530 mW and PS=44.7P_S = 44.7PS=44.7 mW. In order to achieve the maximum modulation instability (MI) gain, the signal wavelength is selected at the peak of the MI gain band. This corresponds to a value of α=0.25\alpha = 0.25α=0.25, which is the dimensionless parameter used in the standard Akhmediev Breather (AB) theory [16]. This wavelength is experimentally determined from MI spectra recorded without launching the signal into the fiber, i.e., under noisy initial conditions.

Special care is taken to maintain constant power levels of both waves during wavelength sweeping (with maximum fluctuations of 0.3 dB). Before investigating the role of third-order dispersion (TOD) in the Fermi–Pasta–Ulam (FPU) process, we ensured that our experimental setup allows the observation of a “standard” FPU recurrence in optical fibers, as reported in Refs. [4,5].

To do so, we first identify a configuration in which the effect of TOD is negligible. The pump wavelength is fixed sufficiently far from the fiber’s zero-dispersion wavelength (ZDW) so that the dispersion can be assumed constant over the entire spectrum. Figure 1(b) illustrates the evolution of the spectrum along the fiber length. An immediate observation is that the spectrum is nearly symmetric on both sides of the pump wavelength, as expected from the theory based on the nonlinear Schrödinger equation (NLSE) [9]. This confirms that a configuration with negligible TOD influence has been achieved.

A second important observation is that the MI process naturally evolves into an FPU recurrence as the fiber length increases. The energy, initially confined to the pump and signal waves [see the input spectrum in Fig. 1(c)], is progressively transferred to harmonics of the signal on both sides of the pump [Figs. 1(b) and 1(d)]. For a clearer understanding, Fig. 1(d) shows the evolution of the signal and pump powers as a function of fiber length.

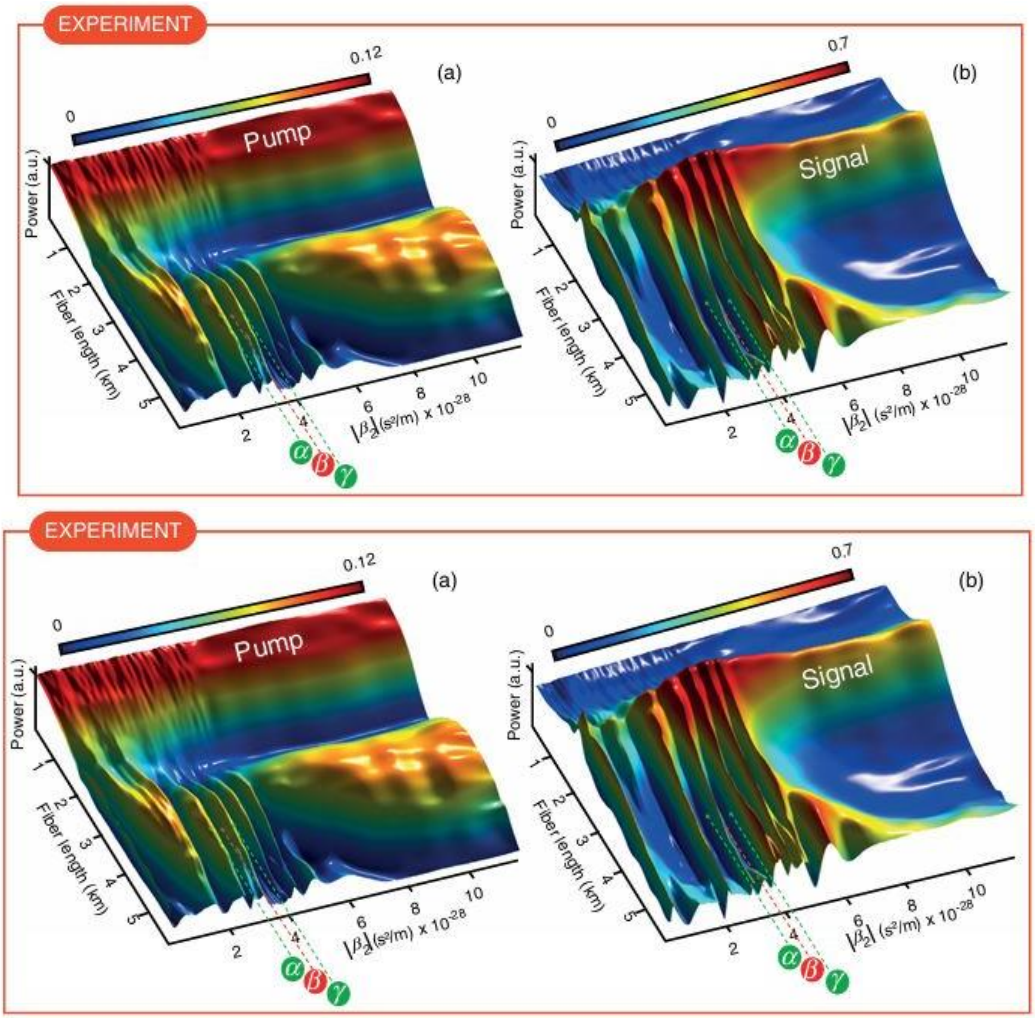
The maximum energy transfer reaches 92% at L=2000L = 2000L=2000 m, with only 8% of the energy remaining in the pump. At this point, the signal power is maximal and the spectrum is the broadest, with more than six harmonics generated on each side of the spectrum (see the red curve in Fig. 1(d)). After this point, the energy transfer reverses, and the process begins to return energy back toward the pump.

To investigate the influence of TOD, the pump wavelength is then shifted toward the fiber’s ZDW. As a result, the MI spectra, whose bandwidth is inversely proportional to the second-order dispersion, broaden significantly, and the dispersion can no longer be considered constant across the entire spectral range. Therefore, it becomes necessary to include the TOD term in the analysis, as is commonly done in studies of modulation instability in low-dispersion optical fibers [22,24,25].

From this point along the fiber length, the energy begins to flow back from the harmonics to the pump. It reaches approximately 79% of the initial pump power at L=3600L = 3600L=3600 m (see Fig. 1(e) and the blue curve in Fig. 1(d)). This high value indicates that the FPU process is highly efficient. Indeed, considering only linear losses, the pump power after propagation over 3600 m of fiber would be expected to be about 84% of its initial value.

Thus, one full cycle of the process is observed, where energy flows from the pump to the sidebands and then back again, forming a recurrence cycle. We observe approximately one and a half periods of recurrence, consistent with the original work of These experimental results are well supported by realistic numerical simulations performed through the integration of the generalized nonlinear Schrödinger equation.

Here, β2,β3,β4\beta_2, \beta_3, \beta_4β2,β3,β4 represent the second-, third and fourth-order dispersion terms, respectively; γ\gammaγ is the nonlinear coefficient of the fiber; and hR(t)h_R(t)hR(t) denotes the Raman response obtained from experimental measurements. The numerical integration is performed using an adaptive split-step Fourier method [35], with a precision of 10−710^{-7}10−7.



We use parameters that are close to the experimental conditions:

b2ðlPÞ¼−100×10−29 dan −1×10−29 s2=m (200 qadam), b3ðlPÞ¼1,2×10−40 s3=m, b4ðlPÞ¼−2,5 ×10−55 s4=m, g ¼2,4=Vt=km, fiber length L ¼ 6000 m, chiziqli zaiflashuv a ¼ 0,2 dB=km, PP¼530mVt va PS ¼ 44,7 mVt.

Although no adjustable fitting parameters were used, excellent agreement with the experimental results is achieved. In addition, the onset of the second recurrence period occurs at L=3000 mL = 3000 \ \text{m}L=3000 m in simulations, compared to L=4000 mL = 4000 \ \text{m}L=4000 m in the experiment. This slight discrepancy can be attributed to uncertainties in pump power measurements, longitudinal fluctuations of dispersion, and/or polarization mode dispersion in the real fiber.

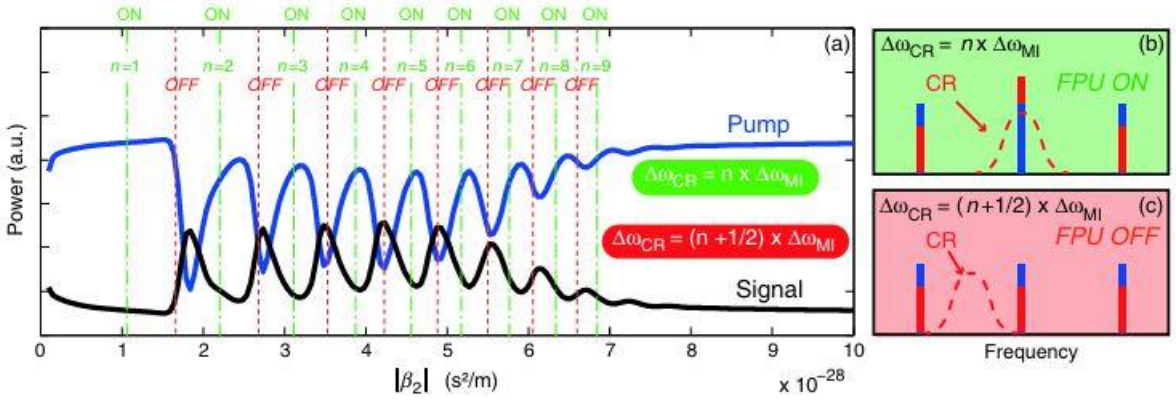
$$\frac{\partial E(z,\tau)}{\partial z} = -i\frac{\beta_2}{2}\frac{\partial^2 E(z,\tau)}{\partial \tau^2} + \frac{\beta_3}{6}\frac{\partial^3 E(z,\tau)}{\partial \tau^3} + i\frac{\beta_4}{24}\frac{\partial^4 E(z,\tau)}{\partial \tau^4}$$
$$+ i\gamma|E|^2 E(z,\tau) + i\gamma\int h_R(t)|E(z,\tau-\tau')|^2 d\tau' E(z,\tau),$$

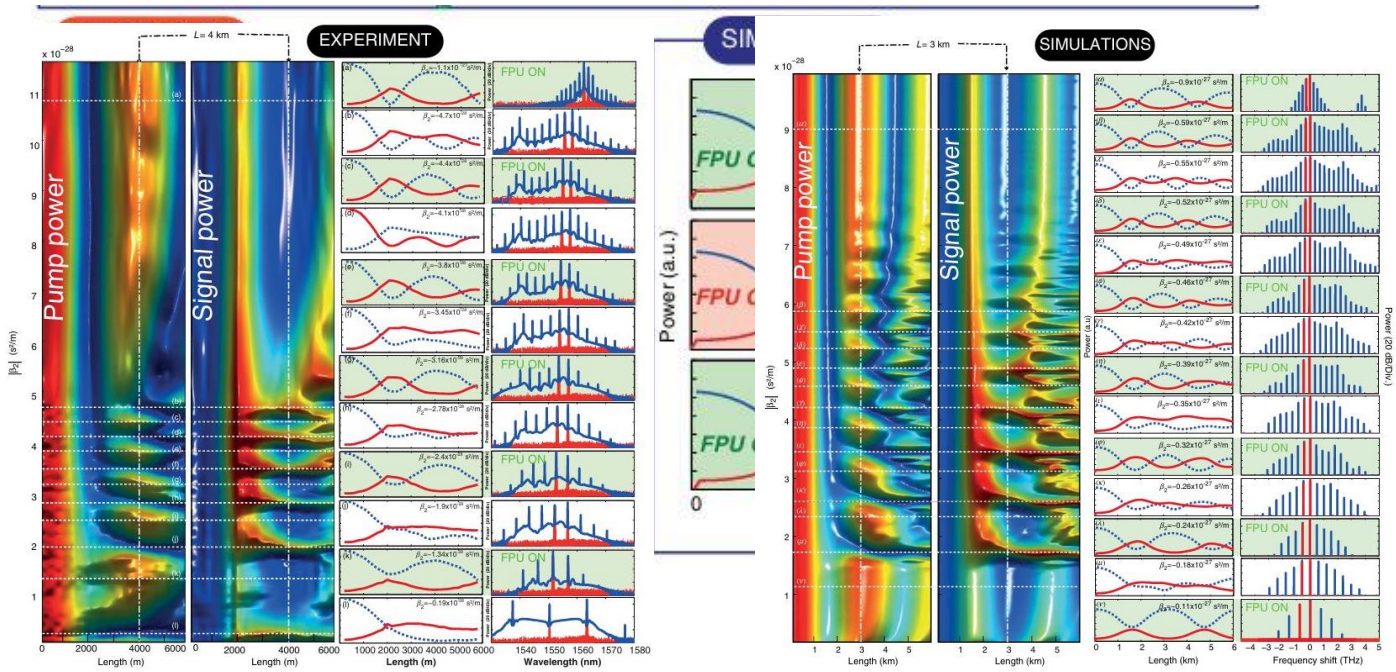
In a previous theoretical study by one of us (see Ref. [26]), it was predicted that the FPU recurrence process would vanish under the influence of dispersion slope and reappear in the very low-dispersion regime. In the present work, we find that the dynamics are significantly more

complex, as there exists a range of |β2|\beta_2||β2| values where the behavior changes qualitatively.

Figure 3: (a) Evolution of the pump power (solid blue curve) and the first harmonic power (solid black curve) as a function of second-order dispersion values. The green vertical lines indicate the |β2|\beta_2||β2| values where Cherenkov radiation (CR) is precisely phase-matched with the modulation instability (MI) harmonics, while the red dotted lines indicate the |β2|\beta_2||β2| values where CR is located between two harmonics. The labels “ON” at the top indicate the regions where FPU recurrence is maximized.

(b) Consequence of perfect phase matching between MI harmonics and CR. (c) Phase mismatch case. In (b) and (c), solid curves represent CR spectra. Spectral components shown in blue correspond to the field before CR generation, while red curves represent components after CR generation is irreversible. Conversely, when Cherenkov radiation is generated between two consecutive MI harmonics, a large part of their energy is lost by several reversible four-wave mixing processes [see Here the losses are reversible and this leads to the suppression of the FPU repetition due to the appearance of Cherenkov radiation. This procedure leads to multiple disappearances. Numerical data. Left two columns: incorrect color scheme of the pump and signal powers with respect to the fiber length and dispersion. Third column: evolution of the signal power





(solid red lines) and the dotted blue lines of the pump power with respect to the fiber length for eigenvalues

of the dispersion. Right column: Corresponding spectrum L¼3000m (blue lines) and L¼0 (red lines). The two right light pink panels show the FPU repetition on states, while the white panels show the FPU repetition off states.

CONCLUSION

In conclusion, the dispersion phenomenon in optical fiber communication systems is one of the important physical factors that significantly affects the quality of signal transmission. As a result of dispersion, optical pulses expand in time, which leads to distortion of the signal shape, the appearance of intersymbol interference, and limitations in transmission speed and distance. Especially in high-speed and long-distance transmission systems, the negative effect of dispersion is more pronounced.

The experiment conducted below shows that the main types of dispersion - chromatic dispersion due to materials and waveguide components, modal dispersion, and polarization-modal dispersion - each have different effects on the optical signal, and appropriate technological approaches must be used to reduce them. In particular, although modal dispersion has almost disappeared in single-mode fibers, the problem of chromatic and polarization dispersion remains relevant.

Various advanced methods are widely used to reduce and control dispersion in modern optical communication systems. In particular, dispersion-compensating fibers, optical compensators, fiber Bragg gratings, soliton transmission technologies, and digital signal processing (DSP) methods provide high efficiency. These technologies allow reducing signal distortion, improving transmission quality, and increasing the overall stability of the system. As a result of the analysis, it can be noted that effective dispersion control is of great importance in increasing the throughput of optical communication systems, extending transmission distances, and ensuring high-speed data exchange. In the future, the development of new technologies for reducing dispersion in optical communication systems, the widespread use of artificial intelligence and digital modeling methods will serve the further development of this area. Therefore, in-depth study of the dispersion phenomenon in optical fiber systems and the introduction of effective methods for its reduction will remain one of the important directions for improving modern telecommunications infrastructure.

REFERENCES

1. Akhmediev, N. N. (2001). Nonlinear physics: Déjà vu in optics. Nature, 413, 267.
2. Benjamin, T. B., & Feir, J. E. (1967). The disintegration of wave trains on deep water Part 1. Theory. Journal of Fluid Mechanics, 27, 417.
3. Fermi, E., Pasta, J., & Ulam, S. (1965). In E. Segre (Ed.), Collected papers of Enrico Fermi (pp. 978–988). Italy: Literary Licensing.
4. Gallavotti, G. (Ed.). (2007). The Fermi-Pasta-Ulam problem: A status report. New York: Springer.
5. Taniuti, T., & Washimi, H. (1968). Self-trapping and instability of hydromagnetic waves along the magnetic field in a cold plasma. Physical Review Letters, 21, 209.
6. Van Simaeys, G., Emplit, P., & Haelterman, M. (2001). Experimental demonstration of the Fermi-Pasta-Ulam recurrence in a modulationally unstable optical wave. Physical Review Letters, 87, 033902.

7. Van Simaeys, G., Emplit, P., & Haelterman, M. (2002). Experimental study of the reversible behavior of modulational instability in optical fibers. Journal of the Optical Society of America B, 19, 477.